Strong, Tailored, Biocompatible Shape-Memory Polymer Networks[**]

Christopher M. Yakacki [Dr.],
Research and Development, MedShape Solutions, Inc., Atlanta, GA 30318 (USA)

School of Materials Science and Engineering, The Georgia Institute of Technology, Atlanta, GA 30332 (USA)

Robin Shandas [Prof.],
Department of Mechanical Engineering, University of Colorado, Boulder, CO 80309 (USA)

David Safranski,
School of Materials Science and Engineering, The Georgia Institute of Technology, Atlanta, GA 30332 (USA)

Alicia M. Ortega,
Department of Mechanical Engineering, University of Colorado, Boulder, CO 80309 (USA)

Katie Sassaman, and
Research and Development, MedShape Solutions, Inc., Atlanta, GA 30318 (USA)

School of Materials Science and Engineering, The Georgia Institute of Technology, Atlanta, GA 30332 (USA)

Ken Gall [Prof.]
Research and Development, MedShape Solutions, Inc., Atlanta, GA 30318 (USA)

School of Materials Science and Engineering, The Georgia Institute of Technology, Atlanta, GA 30332 (USA)

Woodruff School of Mechanical Engineering, The Georgia Institute of Technology Atlanta, GA 30332 (USA)

Christopher M. Yakacki: chris@medshapesolutions.com; Robin Shandas: ; David Safranski: ; Alicia M. Ortega: ; Katie Sassaman: ; Ken Gall:

Abstract

Shape-memory polymers are a class of smart materials that have recently been used in intelligent biomedical devices and industrial applications for their ability to change shape under a predetermined stimulus. In this study, photopolymerized thermoset shape-memory networks with tailored thermomechanics are evaluated to link polymer structure to recovery behavior. Methyl methacrylate (MMA) and poly(ethylene glycol) dimethacrylate (PEGDMA) are copolymerized to create networks with independently adjusted glass transition temperatures (T_g) and rubbery modulus values ranging from 56 to 92 °C and 9.3 to 23.0 MPa, respectively. Free-strain recovery under isothermal and transient temperature conditions is highly influenced by the T_g of the networks, while the rubbery moduli of the networks has a negligible effect on this response. The magnitude of stress generation

Correspondence to: Christopher M. Yakacki, chris@medshapesolutions.com.

of fixed-strain recovery correlates with network rubbery moduli, while fixed-strain recovery under isothermal conditions shows a complex evolution for varying T_g. The results are intended to help aid in future shape-memory device design and the MMA-*co*-PEGDMA network is presented as a possible high strength shape-memory biomaterial.

1. Introduction

Shape-memory polymers are a class of smart materials with the ability to change shape on command in response to an environmental stimulus.[1,2] This shape changing capacity has enabled shape-memory polymers to be used in a myriad of potential and practical applications including smart medical devices,[3–5] implants for minimally invasive surgery,[6,7] sensors and actuators,[8,9] and heat-shrink tubing and films.[10] Figure 1 is an example of a prototype shape-memory polymer device for orthopedic fixation. The device was extruded to a smaller diameter at an elevated temperature and cooled to fix its temporary packaged shape. The figure shows the shape-recovery process when heated to body temperature. When compared to other shape-memory materials (Nitinol and ceramics), shape-memory polymers offer many advantages including lower-cost processing, significantly larger recoverable strains,[11] and the capacity to become multi-functional materials.[12,13] For example, polymers can be designed to be bioactive, drug eluting,[14] and/or biodegradable[3] as well as possess shape memory.

The shape-memory cycle consists of first processing or polymerizing the polymer in its permanent shape. The polymer is then mechanically deformed and fixed at a secondary temporary shape where it will remain indefinitely until its intended use. Once exposed to the proper stimulus, the polymer will attempt to return to its original permanent state. The polymer will either return to its original state (free-strain recovery) or generate stress against its external constraints (fixed-strain recovery). It is important to note that in some applications, the shape-memory effect in polymers may be used to generate stress and not physically recover mechanical strains.

Typically, thermal shape-memory cycles are programmed by mechanically deforming a polymer sample above a given transition temperature (T_{trans}), which can consist of a glass transition (T_g) or melting transition (T_m).[15] Shape fixation is achieved by cooling the sample below T_{trans} through a reduction in free volume and micro-Brownian motion associated with T_g[16,17] or the formation of crystalline domains associated with T_m.[15] The shape-memory effect is then activated by reheating the sample back to T_{trans} and is driven by crosslinks within the system. The crosslinks can be either physical (crystalline segregated domains or entanglements in ultra-high molecular weight polymers) or chemical (covalent bonding) and serve to return the polymer back to its original processed shape via entropic elasticity.[12,15, 18,19] Heating of the sample can be achieved through conduction, convection, light,[9,20, 21] infrared radiation,[22] and alternating magnetic fields.[23–25]

Because the shape-memory effect in polymers is not an intrinsic material property, but rather relies on polymer structure and processing, researchers have suggested tailoring of polymers thermomechanics through variation of the monomer type and/or co-monomer ratio.[18,26, 27] Work has also been performed on how thermomechanical processing influences polymer shape memory. For example, the recovery behavior has been shown to be dependent on the deformation temperature.[28,29] However, little work has been performed to link polymer network structure to shape recovery. In a previous study, our group studied the effects of polymer structure in shape-memory polymer stent prototypes on unconstrained free-recovery under isothermal conditions.[7] Baer et al. studied the shape-memory behavior of a series of biomedical Mitsubishi polyurethanes in an effort to compare thermomechanical properties to

recovery.[30] However, full systematic studies linking polymer network structure to recovery have not been performed. The goal of this paper was to systematically investigate the influence of polymer network structure on both free and constrained recovery under isothermal and transient temperature conditions in thermoset shape-memory polymer networks.

2. Results

The MMA-*co*-PEGDMA polymer system was characterized by running dynamic mechanical analysis on a broad range of compositions varying both amount and molecular weight (M_n) of the PEGDMA crosslinking monomer. These compositions consisted of 25, 50, 75, and 100 wt % PEGDMA with M_n equal to 330, 550, 750, and 1000. Figure 2 summarizes the thermomechanical properties of these networks. Figure 2a shows the dependence of T_g on the PEGDMA crosslinking monomer. The T_g of the networks decreased with increasing amounts of PEGDMA. Furthermore, T_g decreases at a faster rate when using higher molecular weight PEGDMA. In the ranges considered, there is a linear correlation between T_g and amount PEGDMA, which is represented by straight lines for each M_n value. The T_g of pure MMA is converged upon as a 0wt% value of PEGDMA is approached for all M_n values. Figure 2b represents how the rubbery modulus is affected by the PEGDMA crosslinker. For all M_n values, the rubbery modulus increases in an exponential fashion with increasing amounts of PEGDMA. Networks with lower M_n values demonstrated higher rubbery moduli and rates of change in moduli.

After basic characterization of the polymer system, tailored networks were created to independently test the influence of T_g and rubbery modulus on shape-memory behavior. Monomer formulations for networks with tuned thermomechanical properties could be calculated using linear interpolation between the linear trend-lines shown in Figure 2. Using this method, six networks were created for subsequent testing and the transition properties of the networks are presented in Figure 3. Figure 3a reveals three networks with increasing T_g of 56, 76, and 92 °C with approximately equal rubbery moduli of 12.8MPa. Figure 3b displays four networks with increasing rubbery moduli of 9.3, 12.8, 17.2, and 23.0 MPa with approximately equal T_g of 76 °C. These rubbery moduli values were chosen to show roughly equal spacing on a logarithmic scale and demonstrate the efficacy of using linear interpolation to derive the polymer formulations. More precise thermo-mechanical values of the 6 networks can be seen in Table 1. It should be noted that the first network in Figure 3b has a slightly lower T_g (72 °C) compared to the remaining three networks, however, this will be shown to have little significance compared to the relatively large difference in rubbery modulus between the networks. The breadth of glass transition for all six networks ranged between 34 and 38 °C.

Free-strain recovery is defined as unconstrained polymer shape change as a function of temperature during transient heating or time during isothermal hold. Figure 4 describes free-strain recovery from a 30% stored compressive strain for all six polymers under transient and isothermal conditions. Figure 4a presents free-strain recovery as a function of temperature for fixed rubbery modulus values and varying T_g. Increasing T_g correlates to an increase in the activation temperature of the polymer, which delays the start of shape recovery during heating. Furthermore, the recovery profiles of the networks remain identical and are essentially separated by the difference in T_g between the networks. Figure 4b presents free-strain recovery as a function of temperature for fixed T_g and varying rubbery modulus. All of the networks activate at reasonably the same temperature with essentially identical recovery profiles. It should be noted that the network with a rubbery modulus of 9.3MPa slightly leads the remaining three networks. Figure 4c presents free-strain recovery as a function of time at T=50°C for fixed rubbery modulus values and varying T_g. Recovery time decreases significantly as T_g is decreased toward the recovery temperature. The network with T_g equal to 56 °C fully recovers within 10 minutes and the network with T_g equal to 76 °C recovers after approximately 100

minutes. However, the network with T_g equal to 92 °C only recovers 20% strain after 600 minutes. Figure 4d presents free-strain recovery as a function of time at T=50 °C for fixed T_g and varying rubbery modulus. Similar to the results in Figure 4b, changes in rubbery modulus have a relatively small influence on recovery time and the networks all recovery after approximately 100 minutes. The recovery profiles show more variance under isothermal testing (Fig. 4d) than compared in transient heating (Fig. 4b). The network with a rubbery modulus of 9.3 MPa leads the recovery profiles followed by the 23.0, 17.2, and 12.8 MPa networks, respectively.

Fixed-strain recovery is defined as the polymer's generation of stress under full deformation constraint as a function of temperature during transient heating or time during isothermal hold. The fixed-strain recovery behavior of the six polymers after a 30% stored compressive strain is described in Figure 5. Figure 5a reveals the generation of stress under constraint during heating for a fixed rubbery modulus and varying T_g. The total generated stress remains constant, while activation temperature increases with increasing T_g. Similar to the free-strain response under the same conditions, the stress recovery profiles of the three networks are nearly identical and are separated by the difference in T_g of the networks. A supplementary figure is available online that superimposes the free-strain and fixed-strain responses of Figure 4a and Figure 5a. Figure 5b demonstrates the generation of stress under constraint during heating for fixed T_g and varying rubbery modulus. The generated stress significantly increases and the activation temperature decreases with increasing rubbery modulus. The stress plateau in Figure 5a and b for all materials is commensurate with the stress required to deform the material 30% at T_g prior to cooling and shape storage. Figure 5c and d present isothermal stress recovery results as a function of time for varying T_g and rubbery modulus, respectively. The results in Figure 5d are directly analogous to the results in Figure 5b. However, the reproducible results in Figure 5c are intriguing because irrespective of glass transition temperature, all three polymers generate similar stress levels and profiles after ten minutes. These seemingly counterintuitive results will be explained in the discussion.

Lastly, a proprietary network with thermomechanical properties that fall within the range of the six tested networks characterized was tested for biocompatibility. The network was tested for cytotoxicity, sensitization, irritation, acute and subchronic toxicity, and genotoxicity under 10993 GLP guidelines and performed with multiple extracts including normal saline, cottonseed oil, and dimethylsulfoxide. The networks received the highest passing scores possible for all tests.

3. Discussion

Shape-memory polymers have been proposed for a myriad of applications ranging from actuators and sensors to biomedical devices. For any commercial application, the polymer's thermomechanics as well as shape-memory effect must be tailored and optimized to meet the required use of the product. However, to the best of the authors' knowledge, there has been no work to investigate the systematic tailoring of a polymer network's thermomechanics and subsequent shape-memory response. The goal of this study was to link network structure in a thermoset shape-memory polymer system to shape-memory behavior to help aid in the design of future shape-memory applications.

Figure 2 is an ideal example of how the thermomechanics of a co-polymer system can be altered by controlling the amount and molecular weight of the crosslinking PEGDMA monomer. The decrease in both T_g and rubbery modulus with increasing molecular weight PEGDMA can be attributed to the spacing between the linear chains built from MMA (i.e., polymethyl methacrylate). With lower molecular weight crosslinking PEGDMA, the chains are linked closer together with a higher degree of steric hindrance and lower chain mobility. Thus, with

an increase in molecular weight, the chain spacing increases, allowing more conformational motion, and resulting in a decrease in both T_g and rubbery modulus. Lastly, it is important to note in regards to Figure 2b that concurrent research by Ortega et al. is being prepared to show that the rubbery modulus of networks will non-linearly reduce to zero as the crosslinking monomer is decreased down to 0wt%. However, in the range of networks in this study, the rubbery modulus maintains an exponential relationship between 25 and 100 wt% PEGDMA.

The tailored glass transition results in Figure 3 are obtained by balancing multiple molecular weight mixtures of PEGDMA in accordance to the empirical relations obtained in the initial characterization of the system (Fig. 2). In general, increasing the weight percent of PEGDMA will decrease T_g and raise the rubbery modulus, while increasing the molecular weight of the PEG unit will lower both T_g and the rubbery modulus. It should be briefly noted that increasing the amount and M_n of the PEGDMA may lead to a small amount of microphase separation of the PEG unit, however, the overall thermo-mechanics of the shape-memory cycle will remain unaltered. The adjustable nature of both T_g and rubbery modulus is critical to the use of shape-memory polymers in biomedical applications, although this caveat is often not emphasized when new materials are proposed and developed. This allows the mechanical and shape-memory properties of the polymer to be optimized for a given application by tuning the amounts of starting monomer and not introducing any new monomers or additives into the system.

Adjustments in T_g have a significant impact on the free-strain recovery profile of a shape-memory polymer under both increasing temperature and isothermal hold conditions. During heating (Fig. 4a), free-strain recovery initiates near the onset of the glass transition (T_{onset}) when conformational motions are enabled and chain mobility is increased. T_{onset} brings an end to the fixing phase and allows the stored internal stresses of the polymer and thermodynamic increase in entropy to drive shape recovery back to the polymers original undeformed state. [18,31] Provided T_g is constant, the rubbery modulus, which is indicative of the crosslink density, has minimal influence on free-strain recovery behavior during heating over the modulus range considered. The network with the lowest rubbery modulus (9.3 MPa) in Figure 4b has a slightly faster recovery response compared to the other networks and is an artifact of a slightly lower T_g (see Table 1).

Free-strain recovery results as a function of time at a constant temperature also demonstrate a strong influence from T_g but not rubbery modulus (Fig. 4c and d). These results are driven by the visco-elastic nature of the recovery process, and rapid recovery is only induced at temperatures near or above T_{onset} when the polymer has been deformed at T_g. The polymer with a T_g at 92 °C still experiences some recovery (~20%) at 50 °C, indicating the presence of some visco-elasticity well below T_{onset}. Previous work has shown that the crosslink density of networks were highly influential on isothermal free-strain recovery.[7] In the previous study, networks were tested with a much lower crosslinking density with rubbery moduli ranging from 1.5MPa to 11.5 MPa. However, the relative difference in crosslinking density in the present materials is insufficient to observe a significant crosslinking effect on free-strain recovery. This suggests that increasing crosslinking density has a diminishing effect on free-strain recovery, and that differences in free-strain recovery will only be observed at extreme differences in crosslink density.

In contrast to free-strain recovery, fixed-strain recovery is extremely dependent on the rubbery modulus. In fact, the recoverable stresses are directly proportional to the network stresses during initial deformation, which are internally stored into the polymer upon the cooling/ fixation process.[32] The recoverable stress can be approximated by multiplying the rubbery modulus by the imposed strain. Since the imposed strain was kept constant at 30%, the recoverable stress under full constraint is always approximately 1/3 of the rubbery modulus for individual materials. The recoverable stress is controlled by thermodynamic driving forces

attempting to return the network to its lowest achievable entropy state dictated primarily by the shape formed during polymerization. Networks with higher crosslinking densities have larger driving forces to return to their lowest entropy state according to the theory of rubbery elasticity. Consistent with free-strain recovery tests, the results also indicate that complete stress recovery is possible and the networks are not experiencing plasticity. The bounded nature and predictability of the recoverable stress is paramount for applications where controlled forces are necessary.

Although the link between network structure and the final magnitude of generated stress in fixed-strain recovery is clear, the thermomechanics of stress recovery is complicated by thermal expansion.[33] As such, the fixed-strain activation temperatures and times in Figure 5 must be interpreted with caution. For example, the initial linear slopes in the heated fixed-strain recovery tests in Figure 5a and b are primarily due to thermal expansion. The stress generation due to thermal expansion has a decreasing influence as the material approaches the rubbery state and experiences recovery of the stored rubbery strains. A polymer without stored strains will initially generate thermal stress during constrained heating, but subsequently experiences a stress drop that approaches a negligible level with continued heating. In addition, the results in Figure 5c indicate that samples with vastly different T_g values recover to similar stresses over equivalent time periods, in stark contrast with the free-strain recovery tests in Figure 4c. However, these results can be misleading and need adequate explanation.

Samples experience thermal contraction when cooled below their set/activation temperature. The thermal contraction adds about 1% strain to the starting strain of the samples and can be noticed in Figure 4a and b; the normalized strains are <0 initially. In isothermal tests, water is used to flood an environmental chamber and would wash the sample off of the platen. Therefore, before testing began, the platens were gently lowered to the sample to fix the sample for testing. Ultimately, the higher T_g samples recover similar stresses in Figure 5c not because they are fully activated at this temperature, but because they are stiff at the selected recovery temperature and generate large thermal expansion stresses.

The results in Figure 4 and Figure 5 provide a fundamental link between shape-memory behavior and polymer network structure through systematic variation in T_g and rubbery modulus. For biomedical applications, these results are relativistic since recovery at $T_{body}=37$ °Cmaybe desired in certain applications, and appropriate scaling and time-temperature superposition can be used to predict time/temperature recovery response at 37 °C for networks with various relative thermomechanical parameters. The results in Figure 4 and Figure 5 are limiting behaviors and are useful for characterizing and understanding fundamental structure-property relationships in shape memory polymers. In practical applications, the recovery behavior will always be a synergy between free-strain and fixed-strain recovery and constitutive models must be used to appropriately predict combined recovery response.[33]

Biocompatibility tests were performed to help validate the combination of two biocompatible starting homopolymers to create a non-toxic shape-memory polymer system.[5] Polymethyl methacrylate has had a longstanding history in orthopedic implants[34,35] and contact lenses, while poly(ethy-lene glycol) is commonly being used for hydrogels[36] and drug delivery applications. The use of this MMA-*co*-PEGDMA shape-memory polymer system may be well suited for biomedical applications needing tailored, high strength deployment and mechanical properties.

4. Conclusions

Tailored shape-memory polymer networks can be photo-polymerized from methyl methacyrlate and poly(ethylene glycol) dimethacrylate. The polymer structure relating to glass

transition temperature and rubbery modulus can be controlled by adjusting the amount and molecular weight of the poly(ethylene glycol) dimethacrylate crosslinking monomer. Free-strain recovery was highly dependent on the glass transition temperature of the networks while crosslink density had a negligible effect. Fixed-strain recovery was dictated by the crosslink density (rubbery modulus) of the networks. The polymer system demonstrated good biocompatibility for one network within the composition range of materials characterized in this study.

5. Experimental

Materials

Methyl methacrylate (MMA), poly(ethylene glycol)$_n$ dimethacrylate (PEGDMA) with typical molecular weights of M_n=330, 550, 750, and 1000 (PolySciences; PEG$_{1000}$DMA) and photoinitiator 2,2-dimethoxy-2-phenylacetophenone (DMPA) were all ordered from Aldrich, unless otherwise noted, and used in their as received conditions without further purification.

Synthesis of Polymer Networks

MMA-*co*-PEGDMA networks were synthesized by free radical polymerization using 0.2 to 0.4 wt% of DMPA photoinitiator. Mixtures of the MMA monomer, the PEGDMA crosslinking monomer, and the photoinitiator were injected between two glass slides or in a cylindrical mold depending on the subsequent testing. Polymerization was performed under a 365nm UV lamp (B100AP; Blak-Ray) for 30 minutes. A thermal post-cure was performed at 90 °C for 1 hour to help ensure complete polymerization. During materials discovery and development, polymer networks were synthesized with PEGDMA compositions ranging from 25 to 100 wt% and typical molecular weights ranging from 330 to 1000. Pure MMA was not polymerized due to photopolymerization difficulties. The mixtures with PEGDMA 1000 required heating above room temperature to obtain a solution mixture of the MMA-PEGDMA. Through the characterization of approximately 20 different materials, an empirical relation using linear interpolation was developed that related the materials' glass transition temperatures and rubbery moduli to the weight fraction and molecular weight of PEGDMA crosslinker. An empirical formula was employed for selection of the final six materials for complete shape memory testing and analysis.

Dynamic Mechanical Analysis

Dynamic mechanical analysis (DMA) in tensile loading was used to determine the T_g and rubbery modulus of the networks on a TA Q800 DMA. Rectangular samples with dimensions of $1 \times 5 \times 25$ mm^3 were cut and wrapped on the ends with aluminum foil to prevent grip failure due to thermal expansion during testing. The samples were thermally equilibrated at −75 °C for 2 minutes and then heated to 175 °C at a rate of 3 °C per minute. Testing was performed in cyclic strain control at 0.2% strain. A preload force of 0.001 N and a force track setting of 150% were used. T_g was defined at the peak of the tan delta curve. Samples were run in duplicate, and variations in T_g were within a standard deviation of 3–5 °C. T_{onset} was calculated by the intersecting line method. Because MMA-based systems do not exhibit a plateau in the glassy state, the starting point of the left intersecting line was 50 °C less than T_g while the starting point of the right intersecting line was at T_g. The breadth of the glass transition was defined as twice the difference of T_g and T_{onset}. The rubbery modulus was taken at the lowest point in the rubbery plateau.

Recovery Characterization

Free-strain and fixed-strain recovery were measured as a function of increasing temperature on an MTS Insight micro-mechanical tester equipped with an environmental chamber and a

thermal chamber. Cylindrical samples measuring 10 mm in diameter and 20 mm in length were compressed to 30% strain at a rate of 1×10^{-3} s^{-1} at T_g. Samples were subsequently cooled while maintaining the 30% strain at a rate of 5 °C min^{-1} in the range of 0 °C to −15 °C and held for 20 minutes to completely store the stresses within the sample and ensure the polymer was in its stored strain state. Deformed samples were stored at a temperature of approximately 0 °C To induce transient recovery, samples were heated at a rate of 2 °Cmin^{-1} to 100 °C with and without constraint for fixed-strain and free-strain recovery testing, respectively. Isothermal fixed-strain recovery and free-strain recovery were also measured as a function of time by immersing the deformed and stored samples in a 50 °C water bath.

Biocompatibility Testing

Biocompatibility testing was performed by an independent laboratory, AppTec (St. Paul, MN), to ensure accurate and non-biased results. Samples were machined to 8×16 mm^2 cylindrical samples and cleaned for 1 hour in boiling water. Before testing, samples were sterilized via gamma irradiation at a minimum dose of 25 kGy. Cytotoxicity, sensitization (guinea pig maximization), intracutaneous irritation, acute and subchronic toxicity, and genotoxi-city (bacterial mutagenicity, in vitro mouse lymphoma, and in vivo mouse micronucleus) tests were run according to ISO 10993 GLP standards.

References

1. Wei ZG, Sandstrom R, Miyazaki S. J. Mater. Sci 1998;33(15):3743.
2. El Feninat F, Laroche G, Fiset M, Mantovani D. Adv. Eng. Mater 2002;4(3):91.
3. Lendlein A, Langer R. Science 2002;296(5573):1673. [PubMed: 11976407]
4. Metcalfe A, Desfaits AC, Salazkin I, Yahia L, Sokolowski WM, Raymond J. Biomaterials 2003;24 (3):491. [PubMed: 12423604]
5. Lendlein A, Kelch S. Clin. Hemorheol. Microcirc 2005;32(2):105. [PubMed: 15764819]
6. Baer G, Wilson T, Maitland D, Matthews D. J. Invest. Med 2006;54(1):S162.
7. Yakacki CM, Shandas R, Lanning C, Rech B, Eckstein A, Gall K. Biomaterials 2007;28(14):2255. [PubMed: 17296222]
8. Metzger MF, Wilson TS, Schumann D, Matthews DL, Maitland DJ. Biomed. Microdevices 2002;4 (2):89.
9. Small W, Wilson TS, Benett WJ, Loge JM, Maitland DJ. Opt. Express 2005;13(20):8204. [PubMed: 19498850]
10. Tobushi H, Hara H, Yamada E, Hayashi S. Smart Mater. Struct 1996;5(4):483.
11. Kim BK, Lee SY, Xu M. Polymer 1996;37(26):5781.
12. Behl M, Lendlein A. Mater. Today 2007;10(4):20.
13. Shmulewitz A, Langer R, Patton J. Nat. Biotechnol 2006;24(3):277. [PubMed: 16525386]
14. Wache HM, Tartakowska DJ, Hentrich A, Wagner MH. J. Mater. Sci. Mater. Med 2003;14(2):109. [PubMed: 15348481]
15. Liu C, Qin H, Mather PT. J. Mater. Chem 2007;17:1543.
16. Hayashi S, Kondo S, Kapadia P, Ushioda E. Plast. Eng 1995;51(2):29.
17. Liang C, Rogers CA, Malafeew E. J. Intell. Mater. Syst. Struct 1997;8(4):380.
18. Liu C, Mather PT. J. Appl. Med. Polym 2002;6(2):47.
19. Lendlein A, Kelch S. Angew. Chem. Int. Ed 2002;41(12):2034.
20. Lendlein A, Jiang HY, Junger O, Langer R. Nature 2005;434(7035):879. [PubMed: 15829960]
21. Maitland DJ, Metzger MF, Schumann D, Lee A, Wilson TS. Lasers Surg. Med 2002;30(1):1. [PubMed: 11857597]
22. Koerner H, Price G, Pearce NA, Alexander M, Vaia RA. Nat. Mater 2004;3(2):115. [PubMed: 14743213]

23. Mohr R, Kratz K, Weigel T, Lucka-Gabor M, Moneke M, Lendlein A. Proc. Natl. Acad. Sci. USA 2006;103(10):3540. [PubMed: 16537442]

24. Frimpong RA, Fraser S, Hilt JZ. J. Biomed. Mater. Res. Part A 2007;80(1):1.

25. Buckley PR, McKinley GH, Wilson TS, Small W, Benett WJ, Bearinger JP, McElfresh MW, Maitland DJ. IEEE Trans. Biomed. Eng 2006;53(10):2075. [PubMed: 17019872]

26. Behl M, Lendlein A. Soft Matter 2007;3(1):58.

27. Alteheld A, Feng YK, Kelch S, Lendlein A. Angew. Chem. Int. Ed 2005;44(8):1188.

28. Gall K, Yakacki CM, Liu YP, Shandas R, Willett N, Anseth KS. J. Biomed. Mater. Res. Part A 2005;73(3):339.

29. Liu YP, Gall K, Dunn ML, McCluskey P. Smart Mater. Struct 2003;12(6):947.

30. Baer G, Wilson TS, Matthews DL, Maitland DJ. J. Appl. Polym. Sci 2007;103(6):3882.

31. Ping P, Wang W, Chen X, Jing X. J. Polym. Sci. Part B 2007;45(5):557.

32. Wang W, Ping P, Chen X, Jing X. Eur. Polym. J 2006;42(6):1240.

33. Liu YP, Gall K, Dunn ML, Greenberg AR, Diani J. Int. J. Plast 2006;22(2):279.

34. Passy S. Int. J. Cosmetic Surg. Aesthet. Dermatol 2003;5(2):193.

35. Vallo CI. Polym. Int 2000;49(8):831.

36. Baroli B. J. Chem. Technol. Biotechnol 2006;81(4):491.

Figure 1.
Demonstration of a shape-memory polymer cylindrical device expanding for soft tissue fixation. Note: Black lines were drawn for visualization.
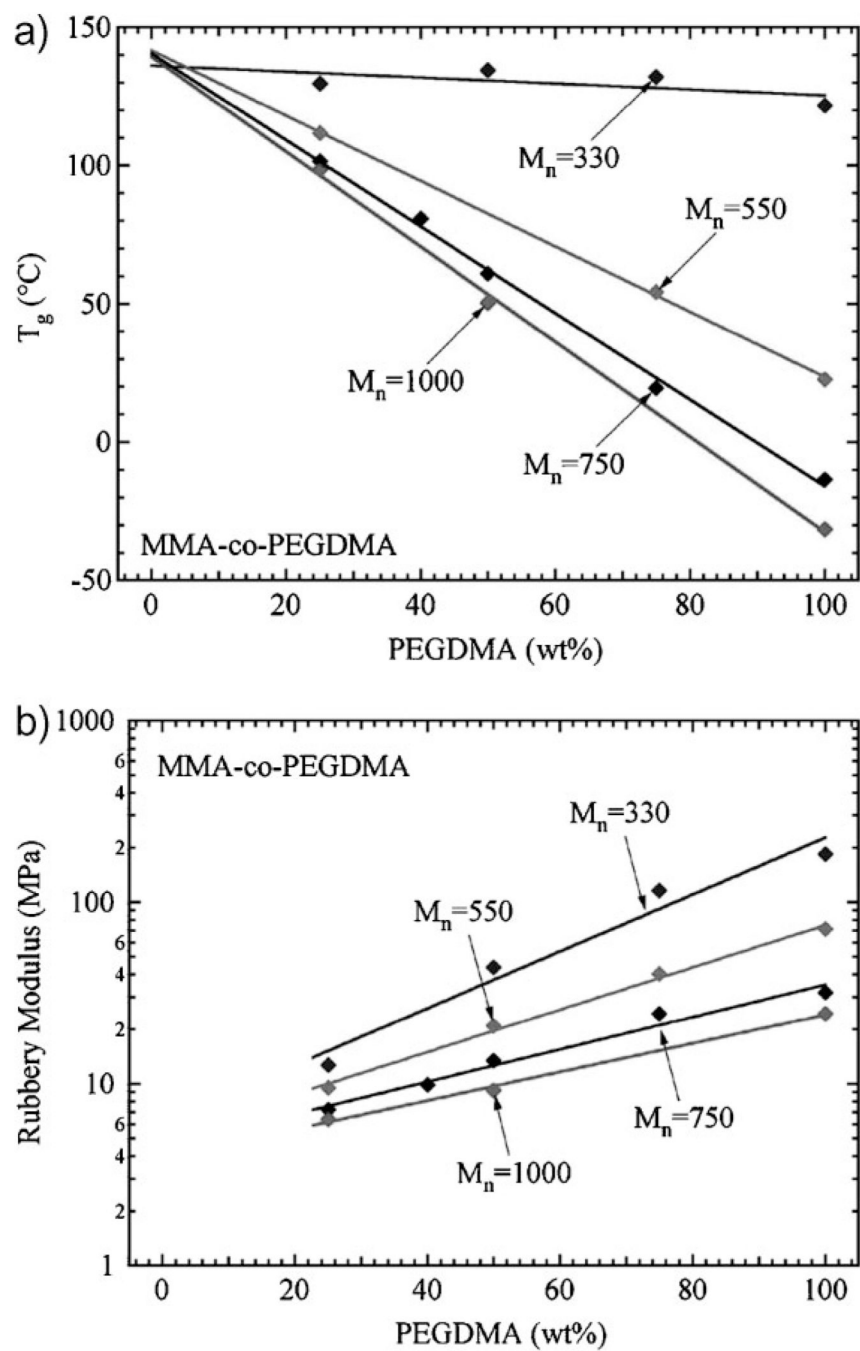
Figure 2.
a). T_g and b). rubbery modulus values for the MMA-co-PEGDMA system as a function of wt % and molecular weight PEGDMA.
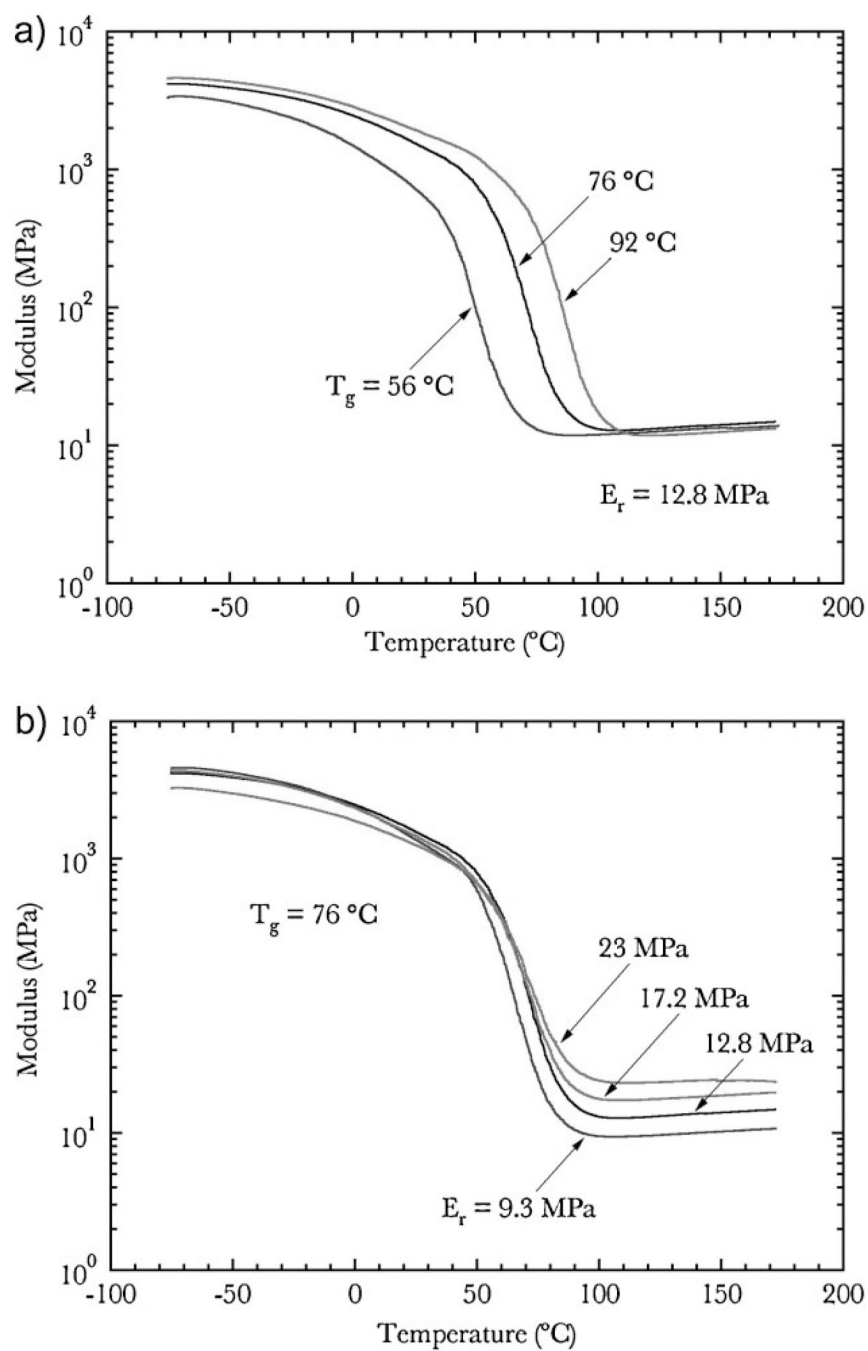
Figure 3.
Glass transitions of custom tailored networks with a). varying T_g and constant rubbery modulus and b). varying rubbery modulus and constant T_g.
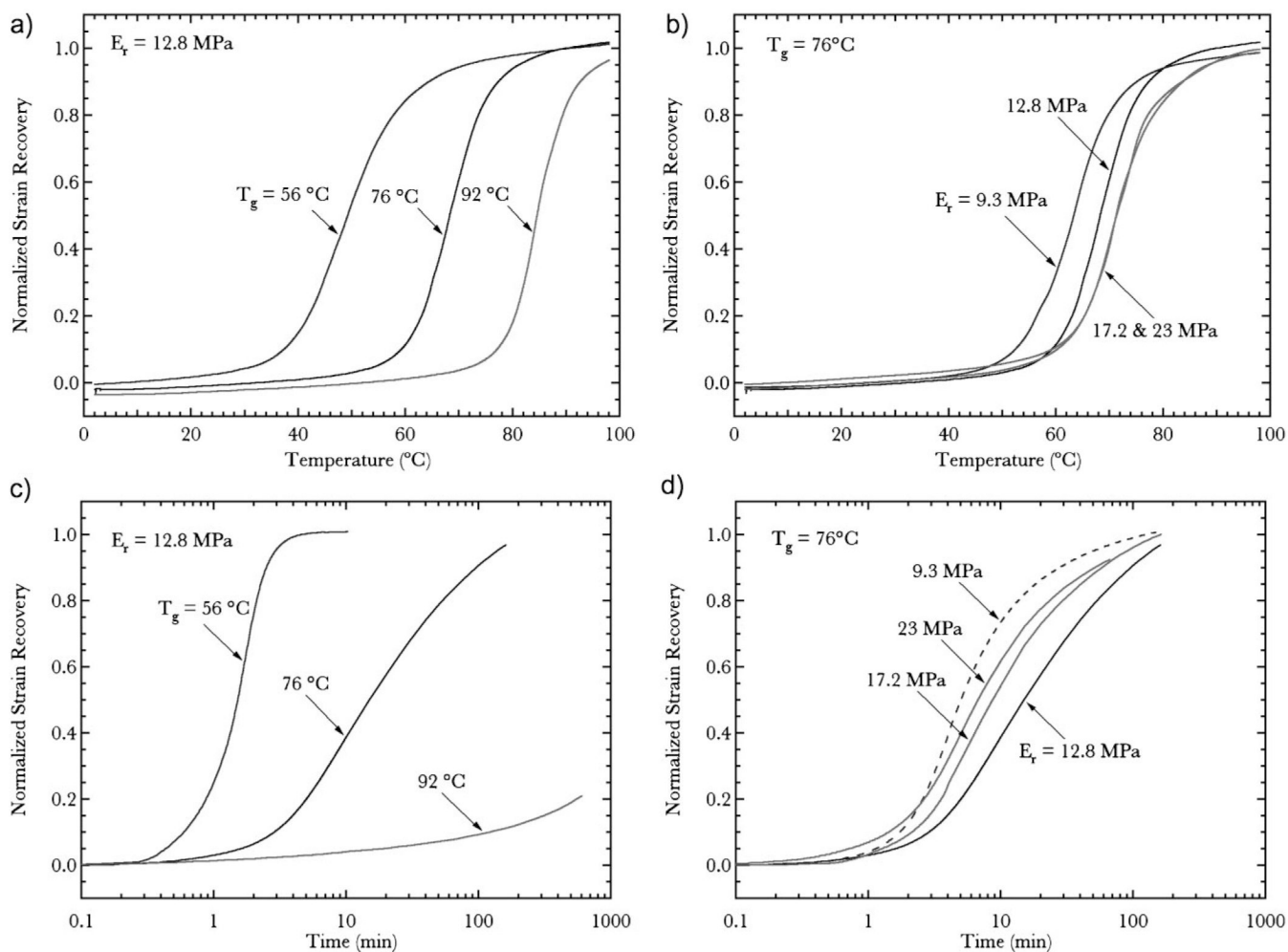
Figure 4.
Free-strain recovery data as a function of temperature for the six materials represented in Figure 3. Specific graphs indicate a) strain recovery as a function of temperature for varying glass transition, b) strain recovery as a function of temperature for varying rubbery modulus, c) strain recovery as a function of time at T=50°C for varying glass transition, d) strain recovery as a function of time at T=50°C for varying rubbery modulus. Normalized strain recovery=ε/ε_{max}.
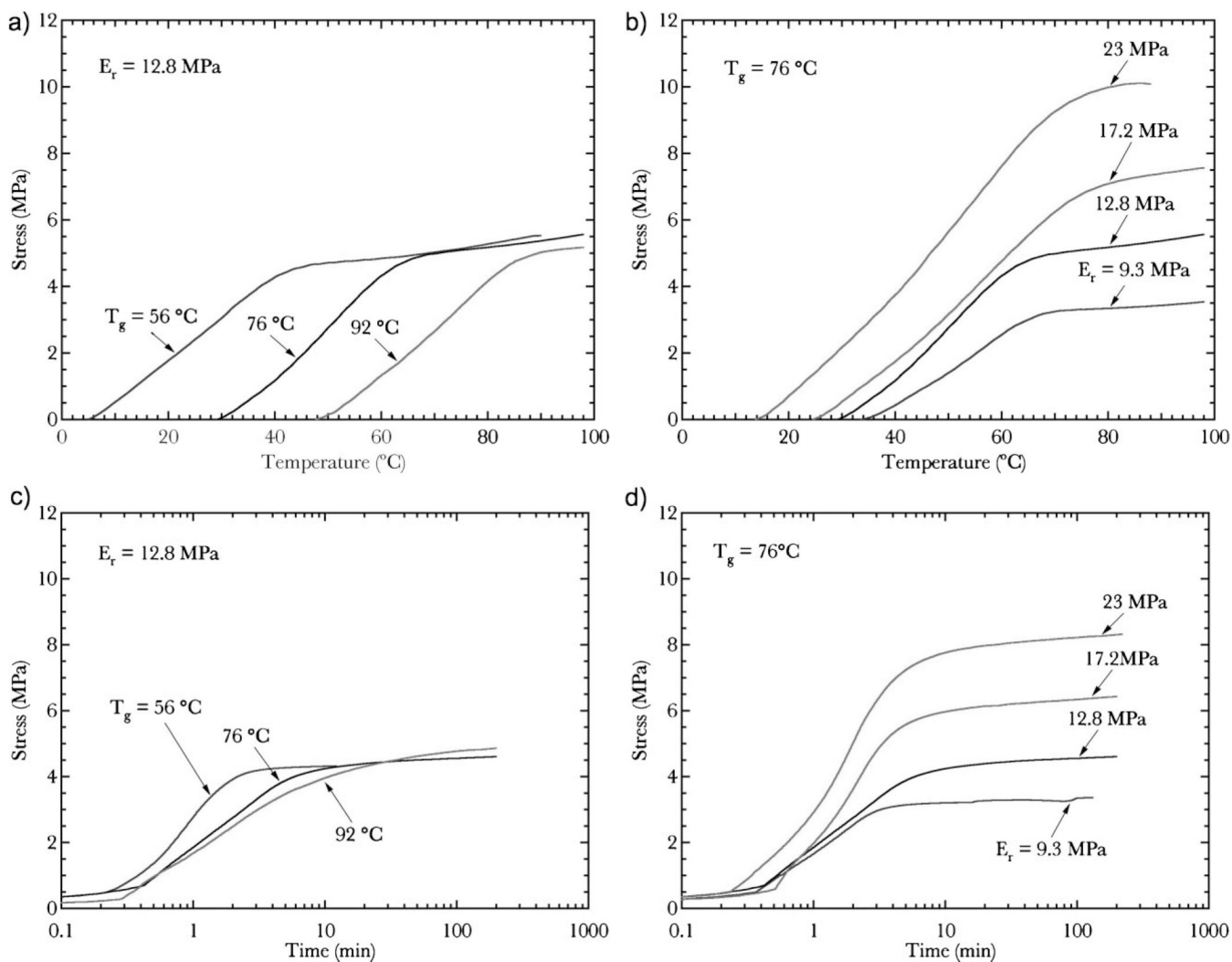
Figure 5.
Fixed-strain recovery data as a function of temperature for the six materials represented in Figure 3. Specific graphs indicate a) stress recovery as a function of temperature for varying glass transition, b) stress recovery as a function of temperature for varying rubbery modulus, c) stress recovery as a function of time at T=50 °C for varying glass transition, d) stress recovery as a function of time at T=50 °C for varying rubbery modulus.

Table 1

Summary of thermomechanical properties of the six networks studied.

	Network	T_g (°C)	E_r (MPa)	T_{onset} (°C)	Breadth of T_g (°C)
Adjust T_g	1	56	12.6	39	34
	2	76	12.8	59	34
	3	92	11.3	75	34
Adjust E_r	1	72	9.3	53	38
	2	76	12.8	59	34
	3	77	17.2	58	38
	4	78	23.0	60	36